Dual-Iron Source Engineering for Optimised Solid-State Reaction Kinetics Towards High-Performance $Na_4Fe_3(PO_4)_2P_2O_7$ Cathode

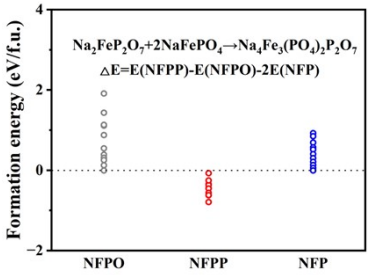

Figure S1. Comparison of the formation energies of NFPP, NFPO and NFP.

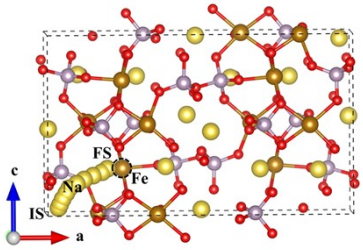

Figure S2. Schematic of Na^+ migration pathways.

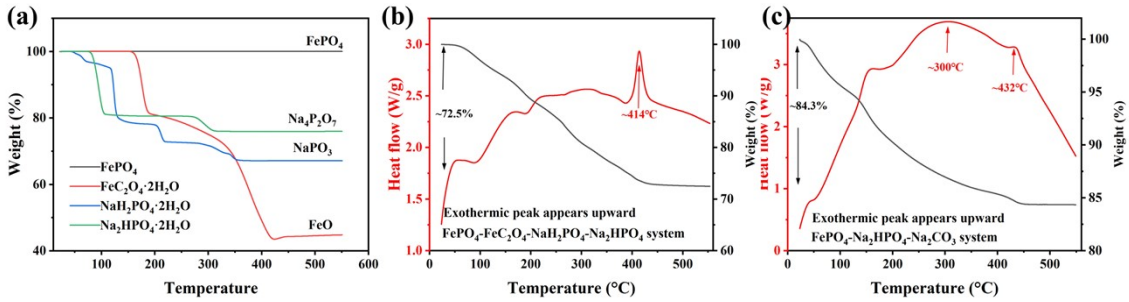

Figure S3. (a) TG curves of the individual starting materials; TG-DSC curves of the precursors during heating: (b) dual-iron-source system; (c) single-iron-source system.

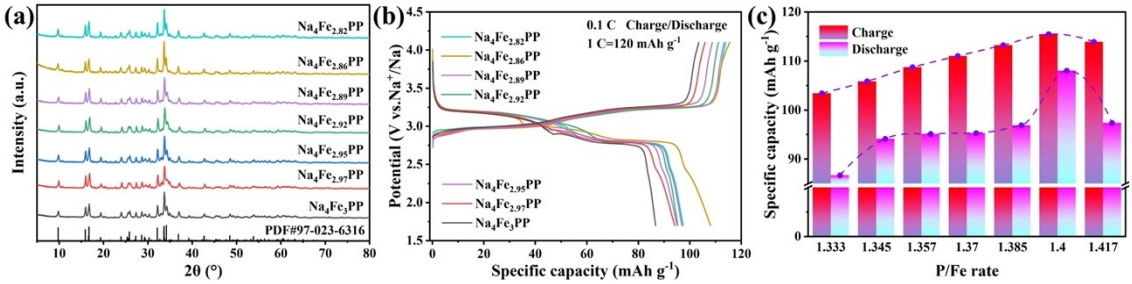

Figure S4. (a) XRD patterns of $Na_4Fe_{3-x}PP$ (x = 0-0.18); (b) Initial charge-discharge curves of the corresponding samples; (c) Variation in charge-discharge capacities.

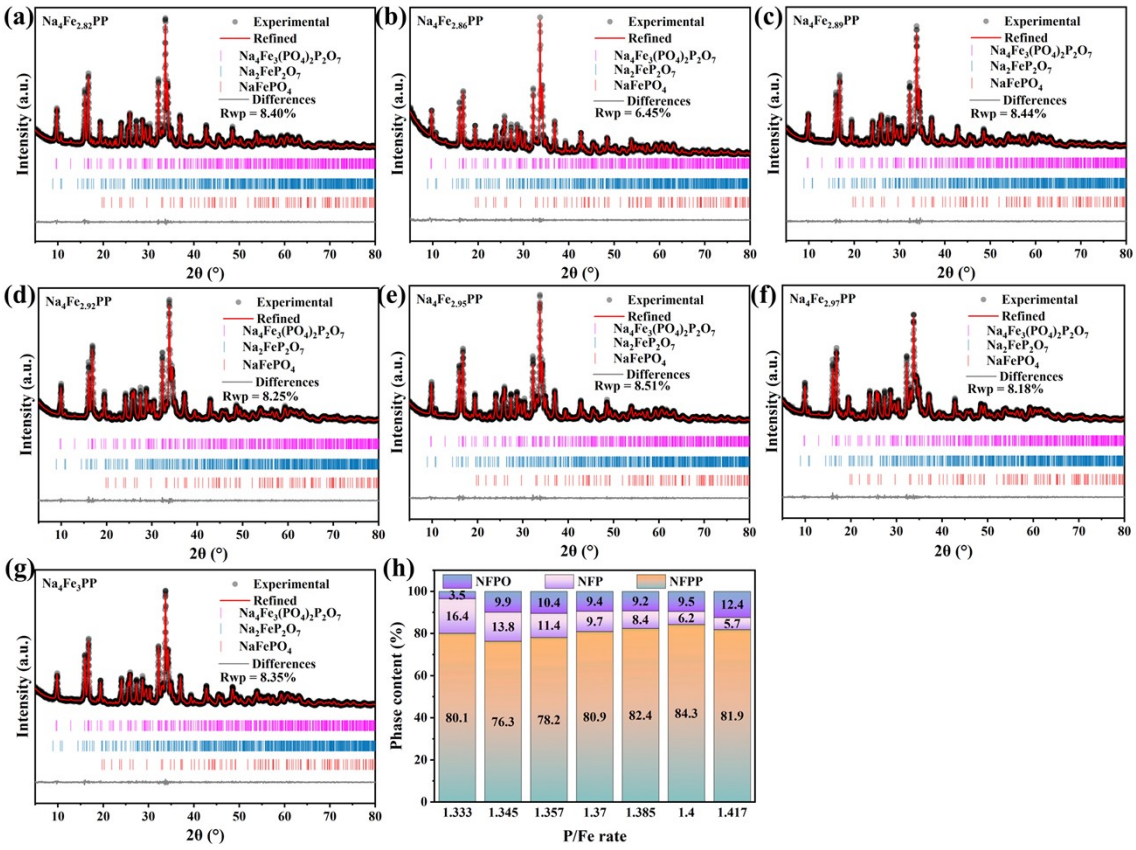

Figure S5. (a-g) Rietveld refinement XRD patterns of $Na_4Fe_{3-x}PP$ (x =0-0.18); (h) Bar chart illustrates the phase composition for each sample.

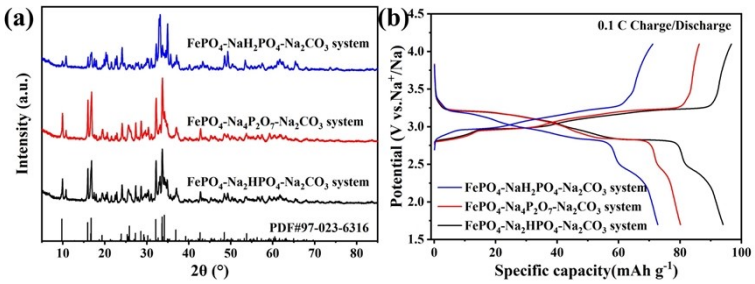

Figure S6. (a) XRD patterns of NFPP samples synthesised using $FePO_4$ as the sole iron source; (b) Initial charge-discharge curves of the various systems.

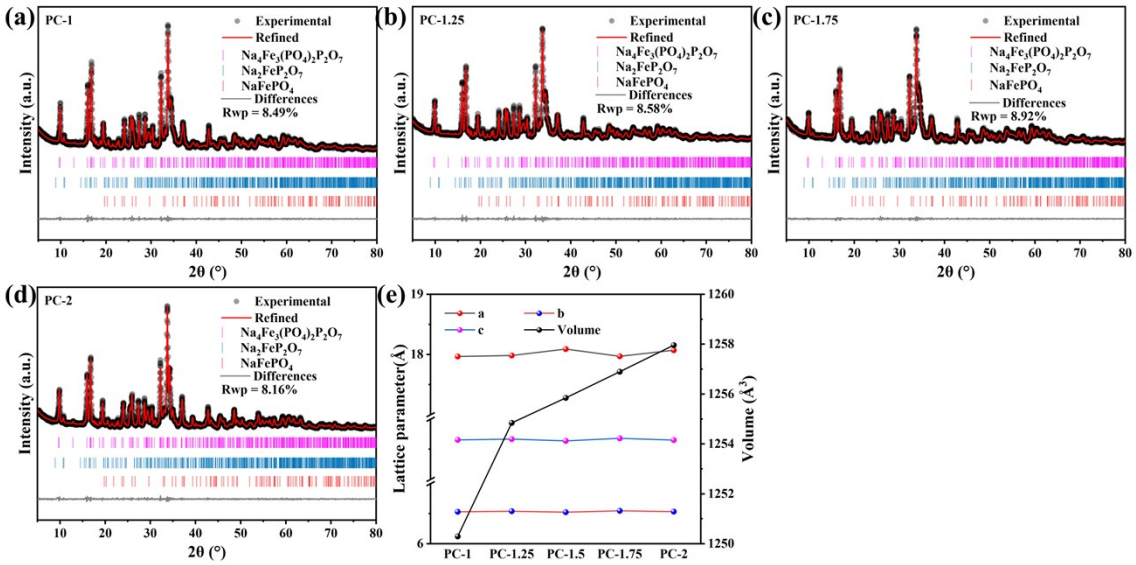

Figure 7. (a-d) Rietveld refinement XRD patterns of PC-y (y = 1, 1.25, 1.75, and 2) ;(e) Variations in lattice parameters and unit-cell volume of PC-y (y = 1, 1.25, 1.5, 1.75, and 2).

Table S1. Detailed structural information of the PC-1 sample following Rietveld refinement.

Formula			**$Na_4Fe_3(PO_4)_2P_2O7$**		
a (Å)			17.96723		
b (Å)			6.53067		
c (Å)			10.65551		
Unitcell volume (Å3)			1250.296		
Atom	x	y	z	Occ	Mult
Fe1	0.338558	0.135247	0.496501	1	4
Fe2	0.139985	0.582787	0.491977	1	4
Fe3	0.255912	0.325017	0.738555	1	4
P1	0.287058	0.592789	0.504229	1	4
P2	0.18296	0.065706	0.480516	1	4
P3	0.56445	0.440303	0.735813	1	4
P4	0.445642	0.128918	0.72551	1	4
Na1	0.507194	0.875136	0.956193	1	4
Na2	0.272013	0.80191	0.734046	1	4
Na3	0.375595	0.366926	0.250438	1	4
Na4	0.447462	0.662449	0.590513	1	4
O1	0.228718	0.553108	0.623639	1	4
O2	0.333516	0.430959	0.46774	1	4
O3	0.338766	0.803239	0.536289	1	4
O4	0.248898	0.605642	0.406926	1	4
O5	0.244214	0.131009	0.623498	1	4
O6	0.116546	0.913994	0.510409	1	4
O7	0.21456	0.064836	0.372994	1	4
O8	0.145408	0.280124	0.461885	1	4
O9	0.488224	0.318952	0.703308	1	4
O10	0.579094	0.553158	0.858391	1	4
O11	0.62266	0.271488	0.746727	1	4
O12	0.581711	0.606387	0.62157	1	4
O13	0.452489	0.1132	0.873315	1	4
O14	0.373682	0.168873	0.687708	1	4
O15	0.482857	0.014463	0.666798	1	4

Table S2. Detailed structural information of the PC-1.25 sample following Rietveld refinement.

Formula			**$Na_4Fe_3(PO_4)_2P_2O_7$**		
a (Å)			17.98338		
b (Å)			6.54053		
c (Å)			10.66854		
Unitcell volume (Å^3)			1254.844		
Atom	x	y	z	Occ	Mult
Fe1	0.338408	0.134902	0.493531	1	4
Fe2	0.140522	0.582218	0.489591	1	4
Fe3	0.257737	0.328423	0.739785	1	4
P1	0.288004	0.57801	0.499972	1	4
P2	0.176262	0.07699	0.48824	1	4
P3	0.565366	0.442595	0.736033	1	4
P4	0.446561	0.129835	0.727173	1	4
Na1	0.505087	0.882829	0.963913	1	4
Na2	0.273164	0.813047	0.748797	1	4
Na3	0.378235	0.379811	0.241151	1	4
Na4	0.454979	0.671285	0.59218	1	4
O1	0.242385	0.552708	0.626535	1	4
O2	0.341408	0.435937	0.468161	1	4
O3	0.325756	0.816906	0.531775	1	4
O4	0.258731	0.631889	0.402374	1	4
O5	0.260665	0.085728	0.607616	1	4
O6	0.117061	0.909692	0.515588	1	4
O7	0.220559	0.052097	0.371265	1	4
O8	0.141219	0.262074	0.465412	1	4
O9	0.478157	0.330182	0.702228	1	4
O10	0.571135	0.563169	0.860148	1	4
O11	0.624411	0.275334	0.747518	1	4
O12	0.588682	0.584915	0.629129	1	4
O13	0.445768	0.105467	0.875276	1	4
O14	0.37109	0.151613	0.677863	1	4
O15	0.485617	-0.00607	0.660765	1	4

Table S3. Detailed structural information of the PC-1.5 sample following Rietveld refinement.

Formula			$Na_4Fe_3(PO_4)_2P_2O_7$		
a (Å)			18.09069		
b (Å)			6.52558		
c (Å)			10.63811		
Unitcell volume ($Å^3$)			1255.851		
Atom	x	y	z	Occ	Mult
Fe1	0.337342	0.132051	0.491971	1	4
Fe2	0.141712	0.582557	0.489598	1	4
Fe3	0.253679	0.32992	0.737456	1	4
P1	0.291359	0.581282	0.502773	1	4
P2	0.179739	0.083651	0.48747	1	4
P3	0.568658	0.441907	0.736094	1	4
P4	0.450784	0.13561	0.728903	1	4
Na1	0.508773	0.861268	0.967738	1	4
Na2	0.275334	0.811068	0.739267	1	4
Na3	0.378532	0.377324	0.235822	1	4
Na4	0.45542	0.679931	0.585203	1	4
O1	0.232465	0.551878	0.606251	1	4
O2	0.339473	0.413751	0.476775	1	4
O3	0.341517	0.77497	0.541662	1	4
O4	0.241336	0.610932	0.386261	1	4
O5	0.237087	0.10479	0.607273	1	4
O6	0.123372	0.899711	0.513086	1	4
O7	0.227263	0.047284	0.37826	1	4
O8	0.135355	0.276023	0.452458	1	4
O9	0.493641	0.3286	0.690118	1	4
O10	0.559377	0.549755	0.859606	1	4
O11	0.623527	0.265344	0.747974	1	4
O12	0.58556	0.583347	0.636922	1	4
O13	0.454765	0.102367	0.880183	1	4
O14	0.367556	0.151413	0.684146	1	4
O15	0.484669	0.006811	0.650364	1	4

Table S4. Detailed structural information of the PC-1.75 sample following Rietveld refinement.

Formula			$Na_4Fe_3(PO_4)_2P_2O_7$		
a (Å)			17.97057		
b (Å)			6.54799		
c (Å)			10.68143		
Unitcell volume (Å3)			1256.897		
Atom	x	y	z	Occ	Mult
Fe1	0.338577	0.135242	0.493949	1	4
Fe2	0.139475	0.578737	0.491661	1	4
Fe3	0.254922	0.333694	0.735279	1	4
P1	0.289215	0.590645	0.507876	1	4
P2	0.179977	0.07997	0.489819	1	4
P3	0.568984	0.440561	0.735496	1	4
P4	0.449487	0.132238	0.725166	1	4
Na1	0.505305	0.878237	0.964902	1	4
Na2	0.271634	0.808423	0.740135	1	4
Na3	0.376224	0.367969	0.24035	1	4
Na4	0.45439	0.677562	0.590472	1	4
O1	0.233752	0.557817	0.623535	1	4
O2	0.337806	0.411147	0.477187	1	4
O3	0.337207	0.7917	0.54815	1	4
O4	0.248632	0.638114	0.383405	1	4
O5	0.242883	0.109674	0.593955	1	4
O6	0.120759	0.908133	0.516655	1	4
O7	0.227317	0.061572	0.373263	1	4
O8	0.134083	0.28204	0.45779	1	4
O9	0.490561	0.34595	0.694129	1	4
O10	0.56083	0.540673	0.851071	1	4
O11	0.62478	0.272006	0.751795	1	4
O12	0.588448	0.601139	0.622562	1	4
O13	0.454301	0.109973	0.869103	1	4
O14	0.375911	0.153449	0.685608	1	4
O15	0.493559	0.004846	0.650535	1	4

Table S5. Detailed structural information of the PC-2 sample following Rietveld refinement.

Formula			$Na_4Fe_3(PO_4)_2P_2O_7$		
a (Å)			18.0708		
b (Å)			6.53523		
c (Å)			10.65195		
Unitcell volume (Å3)			1257.962		
Atom	x	y	z	Occ	Mult
Fe1	0.337485	0.134745	0.491444	1	4
Fe2	0.139918	0.582448	0.49006	1	4
Fe3	0.254871	0.325816	0.738975	1	4
P1	0.29087	0.58396	0.505753	1	4
P2	0.179339	0.072119	0.486515	1	4
P3	0.570207	0.445721	0.736257	1	4
P4	0.449492	0.136347	0.72692	1	4
Na1	0.506507	0.871786	0.966831	1	4
Na2	0.272547	0.804595	0.744289	1	4
Na3	0.378759	0.364586	0.235802	1	4
Na4	0.453335	0.67983	0.589013	1	4
O1	0.233137	0.556644	0.617385	1	4
O2	0.334276	0.427204	0.466666	1	4
O3	0.340179	0.797834	0.533764	1	4
O4	0.243081	0.62588	0.394101	1	4
O5	0.238849	0.113655	0.610383	1	4
O6	0.124866	0.910027	0.513879	1	4
O7	0.225379	0.048939	0.37714	1	4
O8	0.135909	0.281474	0.45485	1	4
O9	0.486545	0.337931	0.694203	1	4
O10	0.561841	0.555101	0.864185	1	4
O11	0.627481	0.271279	0.747559	1	4
O12	0.587564	0.588407	0.625424	1	4
O13	0.458846	0.107486	0.875379	1	4
O14	0.370679	0.155415	0.684729	1	4
O15	0.48611	0.003478	0.657139	1	4

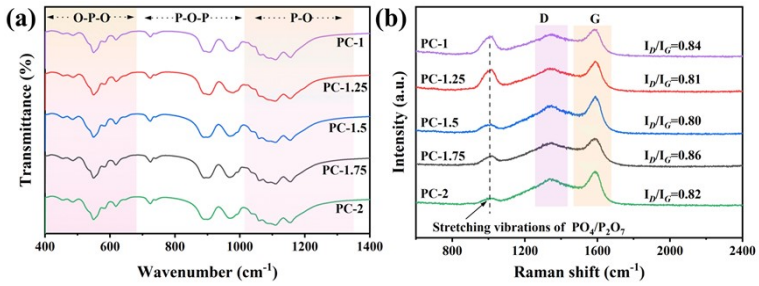

Figure S8. (a) FTIR spectra and (b) Raman spectra of PC-y (y = 1, 1.25, 1.5, 1.75, and 2).

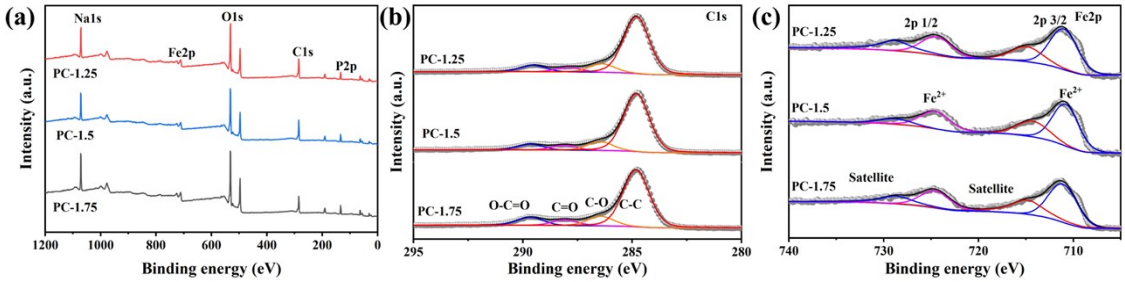

Figure S9. (a) XPS survey spectra of PC-y (y = 1.25, 1.5, and 1.75); (b) High-resolution C 1s spectra of PC-y (y = 1.25, 1.5, and 1.75); (c) high-resolution Fe 2p spectra of PC-y (y = 1.25, 1.5, and 1.75).

Table S6. Carbon content of PC-y (y = 1, 1.25, 1.5, 1.75, and 2) samples determined by a carbon-sulphur Analyser.

Sample	C
PC-2	2.273%
PC-1.75	2.287%
PC-1.5	2.292%
PC-1.25	2.308%
PC-1	2.315%

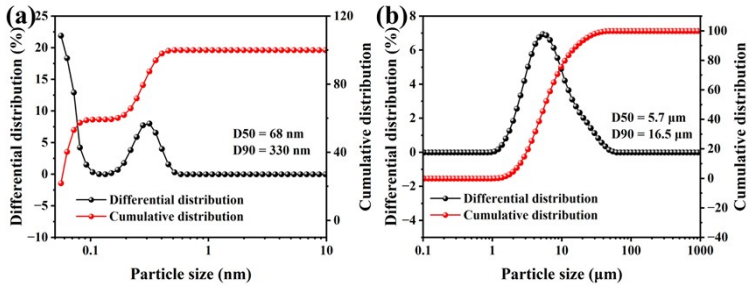

Figure S10. (a) Particle size distribution of the PC-1.5 precursor slurry measured by laser diffraction; (b) particle size distribution of the NFPP measured by laser diffraction.

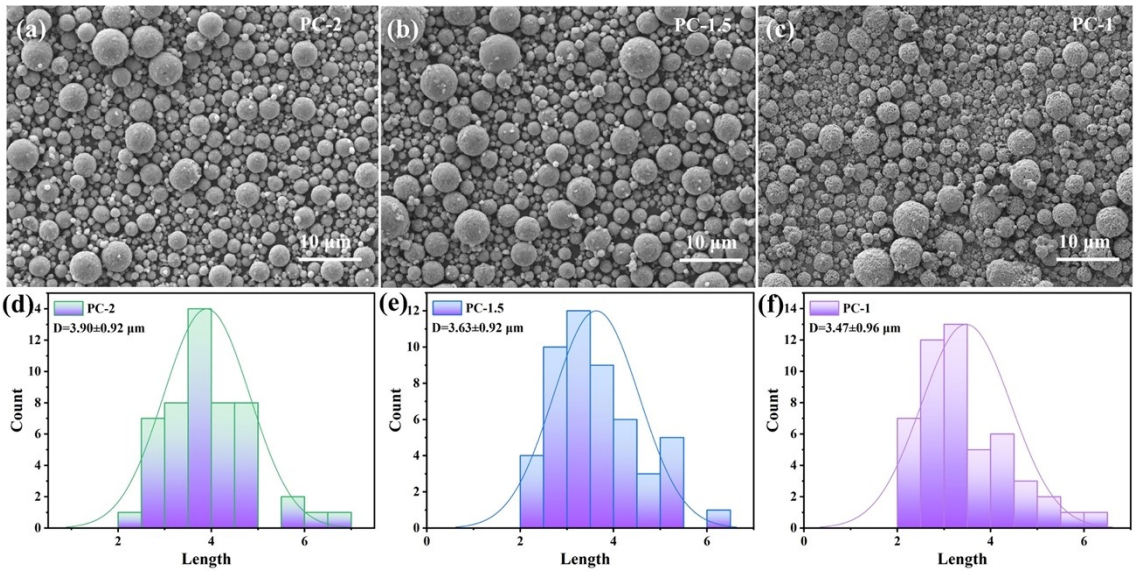

Figure S11. (a- c) SEM images of the PC-y (y = 2, 1.5, and 1); (d-f) Microscopic particle size distributions of PC-y (y = 2, 1.5, and 1).

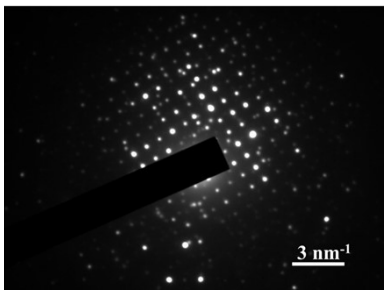

Figure S12. SAED image of PC-1.5.

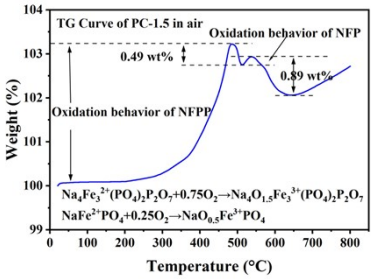

Figure S13.TG curve of the PC-1.5 sample measured in air.

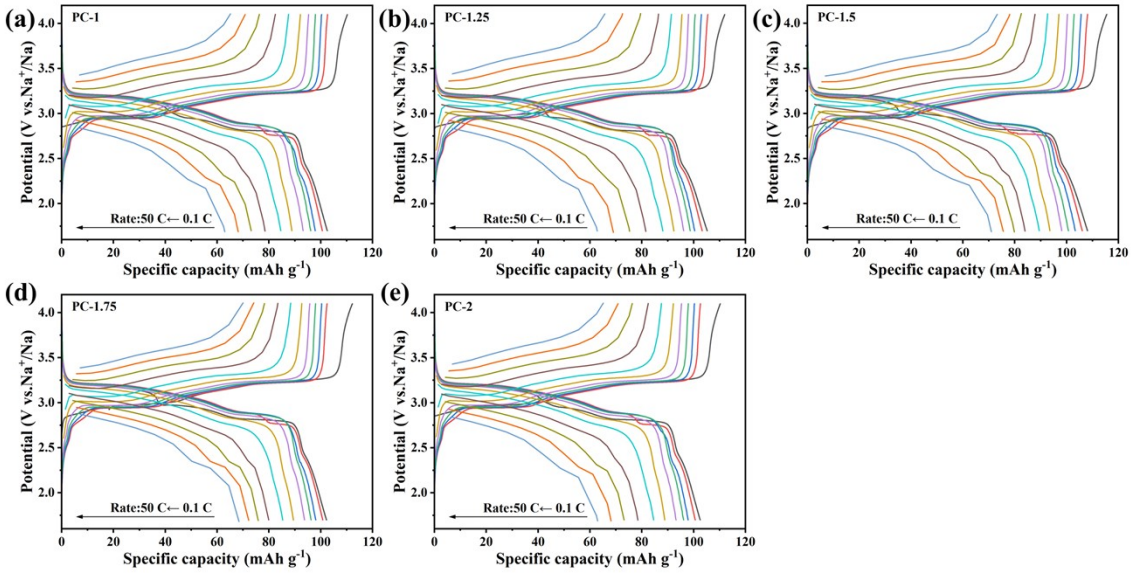

Figure S14. Galvanostatic charge-discharge curves of PC-y (y = 1, 1.25, 1.5, 1.75 and 2) at various current densities.

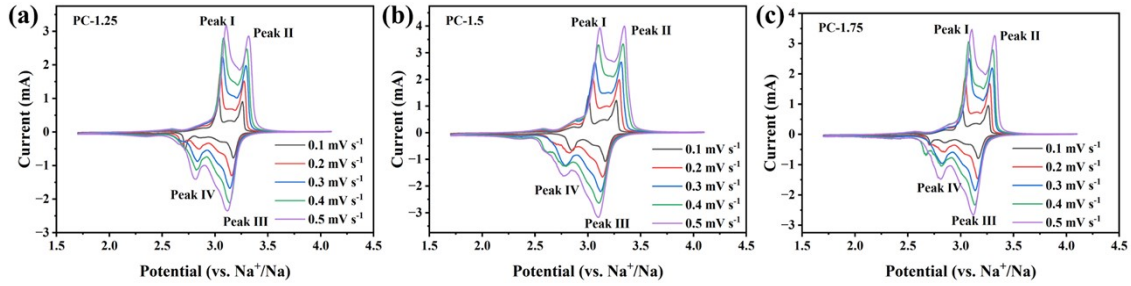

Figure S15. (a-c) CV curves of PC-y (y =1.25, 1.5, and 1.75) at scan rates ranging from 0.1 to 0.5 mV·s^{-1}.

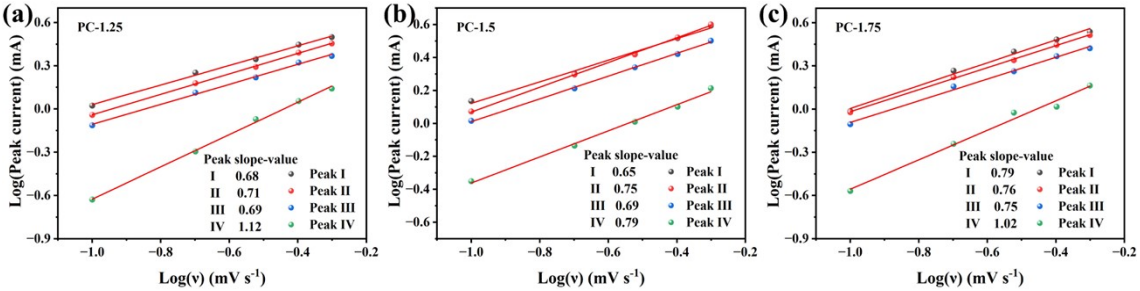

Figure S16. (a-c) The relationship between peak current and the logarithm of the scan rate for PC-y (y =1.25, 1.5, and 1.75).

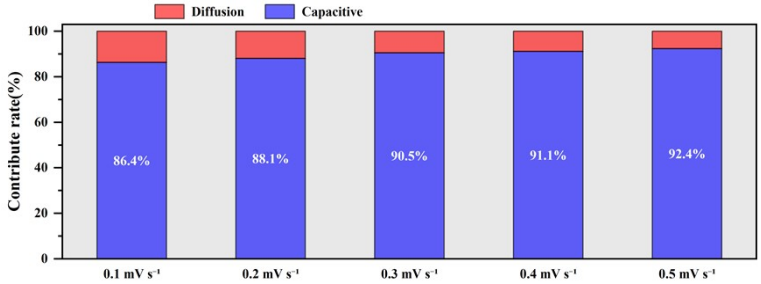

Figure S17. Calculated capacitive contributions at different scan rates.

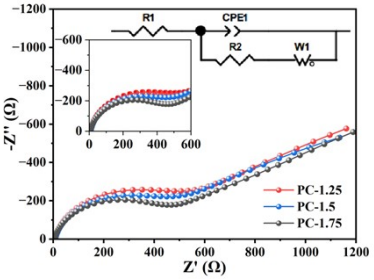

Figure S18. EIS of PC-y (y = 1.25, 1.5, and 1.75).

Table S7. A comparison of the electrochemical performance of NFPP cathodes.

Name	areal loading (mg cm^{-2})	Rate performance	Capacity retention rate/%
$Na_4Fe_{2.91}Co_{0.09}(PO_4)_2P_2O_7$[1]	/	98.5 mAh·g^{-1} at 5 C	80 (6000 cycles) at 20 C
$Na_4Fe_3(PO_4)_2P_2O_7$[2]	/	64 mAh·g^{-1} at 20 C	79.6 (10000 cycles) at 10 C
$Na_4Fe_{2.4}Ni_{0.6}(PO_4)_2P_2O_7$[3]	~ 1.6	86.4 mAh·g^{-1} at 25 C	72.9 (5000 cycles) at 20 C
$Na_4Fe_3(PO_4)_2P_2O_7$–$Na_2FeP_2O_7$[4]	1.2~ 1.4	60.2 mAh·g^{-1} at 200 C	71.4 (10000 cycles) at 50 C
$Na_4Fe_{2.91}Mg_{0.03}Cu_{0.03}Cr_{0.03}(PO_4)_2P_2O_7/C$[5]	~ 2.4	72.4 mAh·g^{-1} at 50 C	79.1 (10000 cycles) at 10 C
$Na_4Fe_3(PO_4)_2P_2O_7$[6]	~ 1.5	87 mAh·g^{-1} at 50 C	81.7 (10000 cycles) at 50 C
$Na_4Fe_3(PO_4)_2P_2O_7$–$Na_2FeP_2O_7$[7]	1.8~ 2	91.4 mAh·g^{-1} at 10 C	77.8 (8000 cycles) at 10 C
$Na_5Fe_{2.9}Ni_{0.1}(PO_4)_2P_2O_7$[8]	/	87.1 mAh·g^{-1} at 10 C	95 (2000 cycles) at 10 C
NFPP/CD[9]	~ 2.1	81.9 mAh·g^{-1} at 50 C	84.4 (6000 cycles) at 20 C
$Na_4Fe_{2.7}Co_{0.3}(PO_4)_2P_2O_7$[10]	~1.25	82.3 mAh·g^{-1} at 100 C	85.6 (5000 cycles) at 10 C
$Na_4Fe_3(PO_4)_2P_2O_7$[11]	~ 2	78 mAh·g^{-1} at 20 C	76.8 (10000 cycles) at 20 C
$Na_{3.6}Fe_{2.6}V_{0.4}(PO_4)_2P_2O_7$[12]	1~2	80.6 mAh·g^{-1} at 50 C	91.3 (11000 cycles) at 30 C
$Na_4Fe_{2.86}(PO_4)_2P_2O_7$ this	~2.7	74.3 mAh·g^{-1} at 50 C	88.7 (6800 cycles) at 50 C

References

1. Y. Cao, X. Xie, Z. Yang, D. Liu, J. Wang, Y. Ma, W. Huang, J. Qin, J. Wang, W. Li and X. Li, *J. Colloid Interface Sci.*, 2025, **703**, 139086.

2. W. Ren, M. Qin, Y. Zhou, H. Zhou, J. Zhu, J. Pan, J. Zhou, X. Cao and S. Liang, *Energy Storage Mater.*, 2023, **54**, 776-783.

3. X. Qi, H. Dong, H. Yan, B. Hou, H. Liu, N. Shang, L. Wang, J. Song, S. Chen, S. Chou and X. Zhao, *Angew. Chem., Int. Ed. Engl.*, 2024, **63**, 202410590.

4. Z. L. Hao, J. Z. Guo, M. Du, X. R. Zhang, Y. L. Heng, Z. Y. Gu, X. T. Wang, X. X. Zhao, N. Yu, Z. H. Xue, S. H. Zheng, B. Li and X. L. Wu, *J. Am. Chem. Soc.*, 2025, **147**, 13905-13914.

5. Q. Lu, T. Shen, Y. Zeng, Y. Zhou, M. Su, Z. Sun, L. Liu, A. Jiang, Y. Wan, Y. Liu and R. Wang, *Adv. Funct. Mater.*, 2025, **35**, 09628.

6. Y. Shao, C. Liu, H. Fan, B. Zhang, L. Liao, A. Zhao, X. Li, P. Chu and Y. Cao, *Small*, 2025, **21**, 2504847.

7. X. Wang, H. Li, X. Ge, L. He, S. Li, Y. Zhang, J. Gu, W. Zhou, Y. Lai and Z. Zhang, *Energy Storage Mater.*, 2025, **79**, 104308.

8. X. Yang, Z. Liu, L. Shi, G. Zhang, J. Liu, H. Huo, B. Qu, S. Lou, L. Zhang and Y. Ma, *Small*, 2025, **21**, 2504863.

9. L. Zhang, R. Sun, Y. Liang, X. Wang, J. Liu, Q. Ning, Q. Yuan, H. He, S. Qiu, Y. Ren, J. Xu and X. Yin, *Energy Storage Mater.*, 2025, **81**, 104548.

10. C. Yang, Y. Ren, B. Wang, H. Luo, W. Liu, Q. Yang, Z. Li, X. Kong, Y. Yao, Y. Yu and D. Zhang, *Advanced Energy Materials*, 2026, **0**, 70907.

11. Q. Xia, L. Zhang, D. Wang, J. Wang, Z. Xu, Y. Zhang, Z. Yao, Y. Guo, P. Jia, L. Zhang and Y. Yang, *Energy Storage Materials*, 2026, **84,** 104849.

12. W. Song, N. Chen, J. Wang, W. Hua, B. Zhang, S. Zhao, X. Ming, Z. Shen, G. Chen and F. Du, *J Am Chem Soc*, 2025, **147**, 39151-39159.